Journal of Biomedical Optics

SPIEDigitalLibrary.org/jbo

Noncontact monitoring of vascular lesion phototherapy efficiency by RGB multispectral imaging

Dainis Jakovels
Ilona Kuzmina
Anna Berzina
Lauma Valeine
Janis Spigulis

SPIE

Noncontact monitoring of vascular lesion phototherapy efficiency by RGB multispectral imaging

Dainis Jakovels,[a,*] Ilona Kuzmina,[a] Anna Berzina,[b] Lauma Valeine,[c] and Janis Spigulis[a]
[a]University of Latvia, Institute of Atomic Physics and Spectroscopy, Biophotonics Laboratory, Raina Boulevard 19, LV—1586, Riga, Latvia
[b]The Clinic of Laser Plastics, Baznicas 31, LV-1010, Riga, Latvia
[c]Beauty Clinic "4th Dimension", Jeruzalemes 1, LV-1010, Riga, Latvia

Abstract. A prototype low-cost RGB imaging system consisting of a commercial RGB CMOS sensor, RGB light-emitting diode ring light illuminator, and a set of polarizers was designed and tested for mapping the skin erythema index, in order to monitor skin recovery after phototherapy of vascular lesions, such as hemangiomas and telangiectasias. The contrast of erythema index (CEI) was proposed as a parameter for quantitative characterization of vascular lesions. Skin recovery was characterized as a decrease of the CEI value relative to the value before the treatment. This approach was clinically validated by examining 31 vascular lesions before and after phototherapy. [DOI: 10.1117/1.JBO.18.12.126019]

Keywords: RGB imaging; erythema index; contrast of erythema index; skin vascular lesions; phototherapy efficiency monitoring; multispectral imaging.

Paper 130602PRR received Aug. 19, 2013; revised manuscript received Nov. 26, 2013; accepted for publication Nov. 27, 2013; published online Dec. 20, 2013.

1 Introduction

The effectiveness of vascular lesion treatment is usually evaluated by visual inspection by a dermatologist. Color images are taken before and after treatment in order to qualitatively assess the results of the treatment; they also serve as evidence in case of complaints.

Several studies of techniques for quantitative assessment of therapy[1] have been performed by laser speckle imaging,[2] laser Doppler perfusion imaging,[3] optical coherence tomography,[4] optical Doppler tomography,[5] reflectance confocal microscopy,[6] pulsed photothermal radiometry,[7] diffuse reflectance spectroscopy, and spectral imaging.[8,9] Skin color image analysis has been offered as a simple and fast method for treatment evaluation,[10,11] but there are some limitations due to errors associated with surface reflection and the effects of skin chromophores other than hemoglobin.[12]

Multispectral imaging can be used for noncontact assessment of skin chromophore (e.g., oxy-/deoxyhemoglobin, melanin) distribution; it reflects the overall skin condition and may facilitate better pathology diagnostics.[13,14] However, commercial multispectral imaging cameras are bulky and expensive, thus limiting their clinical implementation. A digital color RGB camera can be regarded as a low-cost alternative. It acquires three spectral images [red (R), green (G), and blue (B)] simultaneously and can be used as a simple and fast spectral imaging device. In combination with specific narrow-band spectral light sources, RGB imaging could become competitive for some specific applications including the assessment of hemoglobin concentration.[15–18]

Erythema index (EI) is a useful parameter for estimating the cutaneous hemoglobin content and quantitatively characterizing vascular lesions. Simplified methods for determining EI are based on comparing the skin optical density (OD) in green (high hemoglobin absorption) and red (low hemoglobin absorption) spectral ranges.[19] Sometimes EI is attributed also to blood contrast[20] or tissue viability.[16,21] Derma Spectrometer® and Mexameter® are commercially available instruments for point measurements of EI.[22] The contribution of melanin in the skin absorption processes exploited for EI calculations is usually neglected. However, the difference in OD between the blue and green spectral ranges[20] or a weighting factor applied to the absorption index in the red band[23] can be used to correct for the melanin absorption.

EI difference (ΔEI) images representing difference between the port-wine stain (PWS) and normal skin areas were analyzed before and after laser therapy, suggesting that ΔEI may be used as an effective parameter to monitor PWS treatment.[24,25] Imaging techniques support visual inspection of the treatment result and allow spatial analysis of the skin lesion, for example, to compare the area of certain ΔEI threshold level before and after treatment.[24]

Image analysis still requires user-friendly interface improvements before routine clinical use.[1] Dermatologists are interested in a simple, fast, and low-cost technique that supports visual inspection and evaluation of the treatment result.

A handheld prototype RGB imaging system for mapping and monitoring of the hemoglobin distribution in the skin has been designed and tested. The previous study showed that this system can be used to monitor hemoglobin concentration changes during specific provocations such as arterial/venous occlusions and heat test.[17,18] The aim of this study was to clinically test the handheld RGB imaging system for evaluating the vascular lesions' laser and intense pulsed light (IPL) treatment results. The contrast of EI (CEI) was proposed as a parameter for simple and fast quantitative characterization of vascular lesions. The multispectral imaging system was used as a reference.[13]

2 Materials and Methods

2.1 *Data Acquisition*

Measurements were taken with a homemade handheld RGB imaging system [Fig. 1(a)] that consists of a commercial RGB CMOS sensor (USB uEye LE from IDS Imaging

*Address all correspondence to: Dainis Jakovels, E-mail: dainis.jakovels@lu.lv

0091-3286/2013/$25.00 © 2013 SPIE

Development Systems, GmbH, Germany) within a ring of RGB light-emitting diodes (LEDs). Two orthogonally oriented polarizers were placed in front of the CMOS camera and RGB LEDs, respectively, in order to suppress specular reflection from the skin surface.[26] The system was adapted for a working distance of 3 cm, providing a 3×3 cm field of view and a spatial resolution of 0.05×0.05 mm per pixel. The imaging camera was connected to a PC via a USB interface. All settings were manual and were maintained constant during the measurements. Measurements were taken in darkness to reduce artifacts caused by the ambient light. A single measurement lasted <10 s; most of the time was spent for positioning and less than a second for taking a snapshot.

The multispectral imaging system was used as the reference. It consisted of a multispectral imaging camera (Nuance from Cambridge Research & Instrumentation Inc., Woburn, Massachusetts), a halogen lamp ring light, and a pair of crossed polarizers for reducing the specular reflectance. The system was adjusted for a spatial resolution of 0.75×0.75 mm per pixel and a spectral resolution of 15 nm (bandwidth of the Nuance liquid crystal tunable filter). The spectral operating range was 450 to 950 nm.[13] The measurement lasted several minutes—most of the time was spent for positioning and ~1 min to acquire the spectral image cube (51-image stack in steps of 10 nm). The multispectral data were further used for extracting absorption spectra from the regions of interest.

2.2 *Data Processing*

The RGB camera acquired three spectral images simultaneously, where the R channel can be roughly attributed to the 600- to 700-nm spectral range, G to the 500- to 600-nm range, and B to the 400- to 500-nm range. The spectral sensitivity of the RGB imaging system [Fig. 1(b)] was expressed as the product of the spectral sensitivity of the camera and the emission spectrum of the light source.[18]

A registered four-dimensional (4-D) image stack was created in the preprocessing step. The 4-D image stack consisted of two spatial, one spectral, and one temporal dimension. Image registration for each measurement set was performed to compare the data obtained from the measurements. Spatial transformations were performed by manual selection of three control points and using nonreflective similarity transformation. The spectral dimension was created by separating the output signals from the R, G, and B channels of the image sensor. The time dimension consisted of measurements before, directly after, and a month after the treatment.

The EI was used as a parameter for estimating the cutaneous hemoglobin content. The EI can be expressed as a difference in the OD between the green and red spectral ranges of the image detector. The melanin absorption spectrum can be characterized as a curve that descends from blue to red. Therefore, the melanin-corrected EI can be expressed as an OD difference between G and the average value of the B and R channels.[17]

$$\mathrm{EI} = \mathrm{OD}(G) - \frac{\mathrm{OD}(B) + \mathrm{OD}(R)}{2}. \tag{1}$$

The OD that represents absorption can be expressed as

$$\mathrm{OD}(\lambda) = -\log\left[\frac{I(\lambda)}{I_0(\lambda)}\right], \tag{2}$$

where I_0 is the intensity falling upon an object (skin) and I is the intensity of the diffusely reflected light from the skin.

The EI in Eq. (1) can be approximately obtained from the acquired reflectance images (a set of intensity signals I) using Eq. (2).

$$\begin{aligned}\mathrm{EI} &= \log\left[\frac{I_0(G)}{\sqrt{I_0(B)\cdot I_0(R)}}\cdot\frac{\sqrt{I(B)\cdot I(R)}}{I(G)}\right] \\ &= \log\left[k\cdot\frac{\sqrt{I(B)\cdot I(R)}}{I(G)}\right] \approx \frac{\sqrt{I(B)\cdot I(R)}}{I(G)},\end{aligned} \tag{3}$$

where the parameter k was a constant value because all instrument settings were maintained constant during the measurements.

The CEI was proposed as a parameter for quantitative characterization of vascular lesions; it can be expressed as

$$\mathrm{CEI} = \frac{\mathrm{EI}_{\mathrm{std}}}{\mathrm{EI}_{\mathrm{mean}}}, \tag{4}$$

where $\mathrm{EI}_{\mathrm{std}}$ is the standard deviation of EI over the examined area and $\mathrm{EI}_{\mathrm{mean}}$ is the mean value of EI of the same region of interest. The examined area differed from 60×60 pixels to 400×400 pixels depending on the lesion size, but was kept constant within each image stack. The CEI was calculated for each measurement for two regions of interest: the vascular malformation (lesion) and normal skin (reference).

The CEI represents the homogeneity of the hemoglobin content within the region of interest. Higher CEI values are expected for vascular lesions and lower values for normal skin. The

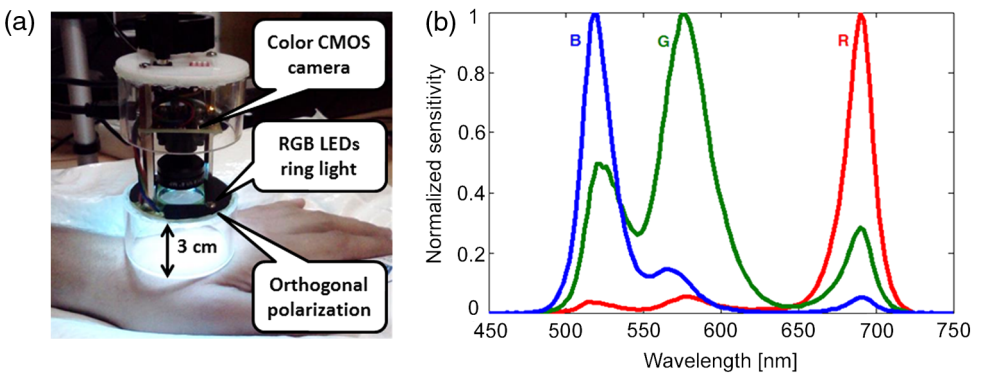

Fig. 1 RGB imaging system: color image (a) and spectral sensitivity of each color channel (b).

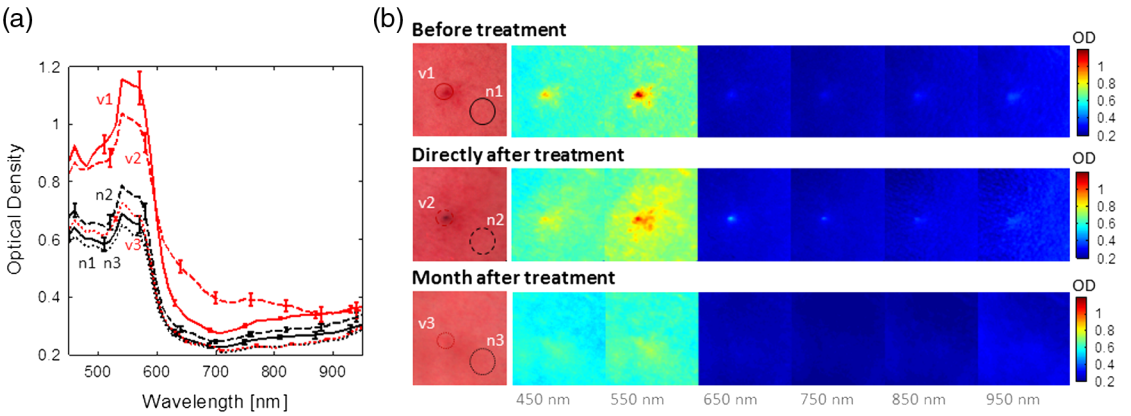

Fig. 2 Optical density spectra (a) before (full line), directly after (dashed line), and a month after (dotted line) treatment of telangiectasia (red) and normal surrounding tissue (black), and corresponding optical density maps (b) at six different wavelengths.

results of the procedure can be assessed quantitatively by comparing the CEI values before and a month after phototherapy.

2.3 *Participants*

Forty-five Caucasian adults (23 to 57 years old) with different skin vascular lesions were voluntarily recruited for the study. Twenty-three hemangiomas, twenty-one telangiectasias, and one PWS were located at different sites of the body. All the subjects studied had Fitzpatrick skin type II. Therapy was performed by IPL (560 nm, 18 J/cm^2), a diode laser (800 nm, 40 J/cm^2), or an Nd:YAG laser (1064 nm, 150 to 180 J/cm^2). The type of phototherapy device and its operating parameters were selected by a dermatologist after visual inspection of the lesion. The dermatologist also gave a subjective evaluation of the result of treatment by rating the improvement as unobservable (no), slight, significant, or very good. The clinical trial was approved by the local ethics committee.

Fourteen lesions were measured before and immediately after therapy, and 31 lesions were measured before, immediately after, and a month after therapy by use of the RGB and multispectral imaging systems. Only the triple-examined 31 lesions were further analyzed.

3 Results

Figure 2 shows a typical vascular lesion telangiectasia (v1) that appears darker and redder compared to the surrounding tissue (n1). A distinctly darker spot can be observed in the center of the malformation. The optical density spectra [Fig. 2(a)] indicate that the increased absorption corresponds to the characteristic bands of hemoglobin between 500 and 600 nm.

The redness of the skin increased in the lesion and its surrounding tissue (n2) after the laser therapy (1064 nm Nd:YAG laser, 160 J/cm^2, 15 ms). OD spectra indicate increased hemoglobin concentration. The center of the telangiectasia (v2) appears darker and changes color to gray or black. Blood vessels are destroyed by phototherapy in this skin region; increased OD values in the range of 600 to 800 nm indicate increased deoxyhemoglobin and methemoglobin concentration levels.[27]

A significant improvement is normally observed within a month after the treatment. The telangiectasia (v3) is barely noticeable to the naked eye, but still has a significantly different spectrum in the range of 450 to 600 nm compared to the surrounding tissue (n3).

The color images of skin before, immediately after, and a month after laser treatment along with the corresponding OD maps are presented in Fig. 2(b). Telangiectasia appears as a spot with a higher OD value. The best contrast between the vascular lesion and the surrounding tissue can be achieved in the green (~550 nm) spectral range, while in the red (~650 nm) spectral channel, absorption and contrast are significantly reduced. Therefore, the difference in OD values between the green and red spectral channels is used to calculate the EI. This parameter represents the cutaneous hemoglobin content but does not provide information about different hemoglobin types and oxygenation.

RGB images with the corresponding EI maps and CEI values of the same case of telangiectasia are shown in Fig. 3(a). The CEI decreased by 50% a month after treatment, and the vascular malformation was no longer visible to the naked eye. Decrease in CEI (for 25%) was also observed directly after treatment, but it was mainly caused by irritation of the surrounding skin.

An example of hemangioma treatment is shown in Fig. 3(b). If compared to the telangiectasia before the treatment, the hemangioma had a contrast of EI three times higher. The treatment was also performed with the 1064-nm Nd:YAG laser (160 J/cm^2, 20 ms), resulting in a 72% reduction of the CEI value. Irritation of the surrounding skin that caused 46% decrease in CEI was also observed.

The average contrast of EI values of all 31 lesions and their surrounding normal skin were calculated [Fig. 4(a)]. The contrast of EI is much higher (on average four times) for vascular malformations compared to the surrounding normal skin. The variation of CEI for vascular malformations is also higher due to different types of lesions. The CEI and its variation tend to decrease after laser treatment by 45%, on average. Related-samples Friedman's two-way analysis of variance test shows that CEI values of vascular lesions before, directly after, and a month after treatment have statistically significant differences ($p < 0.0001$). However, the CEI remained stable (low and small standard deviation) for the surrounding normal skin, except directly after treatment, when irritation of the surrounding tissue occurred. It is possible to determine a clear boundary in CEI between normal skin and vascular lesions (CEI = 0.03) for this study.

A comparison of the CEI values before and a month after treatment is presented in Fig. 4(b). Normal skin measurements (black dots) cluster around a CEI value of ~0.02, but vascular

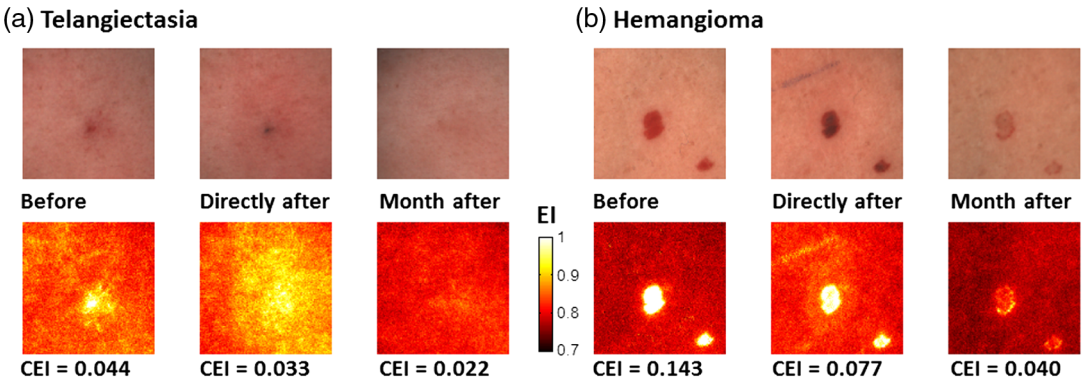

Fig. 3 Examples of telangiectasia (a) and hemangioma (b) before, directly after, and a month after the laser treatment: color images with the corresponding erythema index maps and contrast of erythema index values.

malformations (red dots) have a much higher CEI with values that are widely scattered. The threshold level indicated by the horizontal line at CEI = 0.03 (after treatment) separates the lesions that reached the contrast of normal skin.

Improvement in skin recovery can be presented as a percentage decrease in the CEI by comparing the CEI values before and a month after treatment. A histogram of the improvement in CEI for all 31 lesions is shown in Fig. 5(a). One case [Fig. 5(b1)] did not show improvement; this lesion was a pathology that appeared as a PWS. Up to 10% improvement in CEI was found in three cases [two of them are shown in Figs. 5(b2) and 5(b3)]. The dermatologist rated these four cases as no improvement. Slight improvement (10 to 30%) was found in six cases and significant improvement (30 to 60%) in seven cases. Seven treatments showed very good improvement (>60%), and of these, the largest value for improvement in CEI was 79%. The same ratings were received from the dermatologist [Fig. 5(a)]. In the case of seven lesions, phototherapy was fully successful, and the vascular lesion totally disappeared; measurements a month after treatment could not be made.

Correcting for the melanin absorption[20,23] does not fully remove the influence of melanin on EI. Reducing melanin

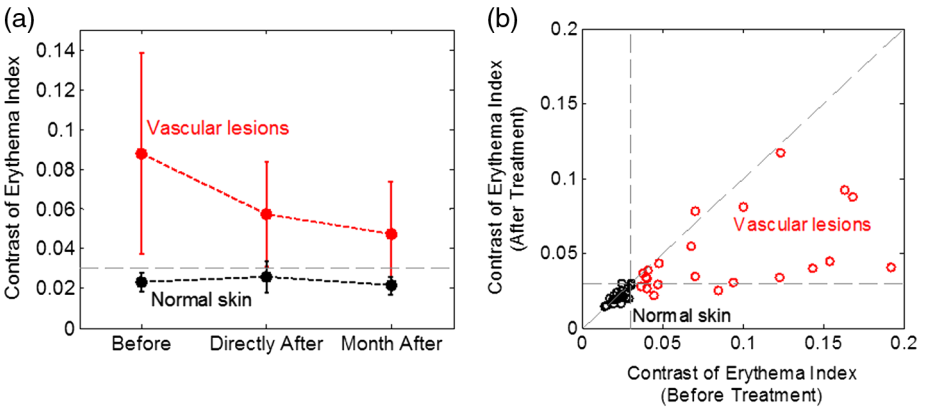

Fig. 4 Average contrast of erythema index (CEI) values of 31 lesions before, directly after, and a month after treatment (a) and comparison of the CEI values before and a month after treatment for all examined lesions (b). The lesions are colored in red, normal skin in black.

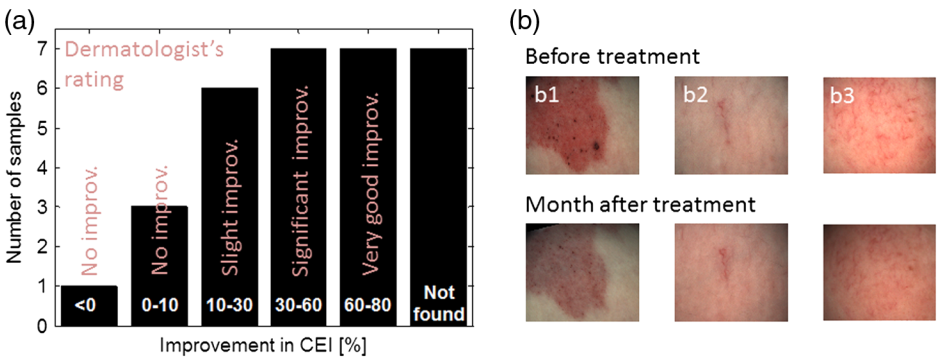

Fig. 5 Histogram of improvements in the CEI of 31 lesions and the corresponding ratings from the dermatologist (a) and color images of unsuccessful treatment samples: port-wine stain (b1), superficial venous network (b2), and telangiectasia (b3).

does help to better highlight vascular features in the EI maps. Along with the previous studies,[24,25] we assume that the epidermal melanin content does not change between the measurements. Patients are usually recommended to avoid tanning and other skin irritating procedures after the treatment. All the subjects studied had Fitzpatrick skin type II, so the skin melanin content was assumed to be similar. Moreover, the CEI of the surrounding normal skin had remained stable with low values and small standard deviation. The influence of different melanin levels on the CEI parameter should be studied further. Additional wavelengths in the infrared spectral range could be used for more precise measurements and for correcting the melanin content.[28]

Our results showed that the measured improvement in CEI corresponded well with the dermatologist's rating and thus, supplemented a qualitative measure of the effectiveness of phototherapy with a quantitative parameter that can be obtained easily from the RGB image data. Further improvements could be the implementation of an RGB imaging device that can be connected to a common clinical device or smartphone.

4 Conclusions

The developed RGB imaging system appeared to be useful for quantitative evaluation of the effectiveness of phototherapy of vascular lesions. The EI was chosen as a parameter for estimating the cutaneous hemoglobin content. The CEI was proposed as a parameter for quantitative characterization of vascular lesions; it represents the homogeneity of the hemoglobin content within the region of interest. The degree of skin recovery is reflected as a percentage decrease in the CEI values before and after phototreatment.

This study demonstrates the potential of a simple RGB imaging technique for implementation in routine clinical praxis. It is a fully noninvasive technology; other advantages of the RGB imaging are small instrument size, good spectral performance, and low equipment cost. The simplicity of computing parameters allows nearly real-time monitoring. The RGB imaging system and algorithm described above could be further implemented as a connection kit to some common clinical device or smartphone.

Acknowledgments

This work has been supported by the European Social Fund within the projects Support for Doctoral Studies at University of Latvia (No. 1DP/1.1.2.1.2./09/IPIA/VIAA/004) and Biophotonics Research Group (No. 2009.0211/1DP/1.1.1.1.2.0/09/APIA/VIAA/077).

References

1. S. A. Sharif et al., "Noninvasive clinical assessment of port-wine stain birthmarks using current and future optical imaging technology: a review," *Br. J. Dermatol.* **167**(6), 1215–1223 (2012).
2. Y. C. Huang et al., "Blood flow dynamics after laser therapy of port wine stain birthmarks," *Lasers Surg. Med.* **41**(8), 563–571 (2009).
3. A. M. Troilius and B. Ljunggren, "Evaluation of port wine stains by laser Doppler perfusion imaging and reflectance photometry before and after pulsed dye laser treatment," *Acta Derm. Venereol.* **76**(4), 291–294 (1996).
4. F. Bazant-Hegemark et al., "Optical coherence tomography: a potential tool for unsupervised prediction of treatment response for Port-Wine Stains," *Photodiagnosis Photodyn. Ther.* **5**(3), 191–197 (2008).
5. J. Nelson et al., "Imaging blood flow in human port-wine stain in situ and in real time using optical Doppler tomography," *Arch. Dermatol.* **137**(6), 741–744 (2001).
6. S. Astner et al., "Preliminary evaluation of benign vascular lesions using in vivo reflectance confocal microscopy," *Dermatol. Surg.* **36**(7), 1099–1110 (2010).
7. W. Verkruysse et al., "Thermal depth profiling of vascular lesions: automated regularization of reconstruction algorithms," *Phys. Med. Biol.* **53**(5), 1463–1474 (2008).
8. I. Kuzmina et al., "Contact and contactless diffuse reflectance spectroscopy: potential for recovery monitoring of vascular lesions after intense pulsed light treatment," *J. Biomed. Opt.* **16**(4), 040505 (2011).
9. B. J. Jung, "Polarization spectral imaging system for quantitative evaluation of port wine stain blanching following laser treatment," *J. Opt. Soc. Korea* **7**(4), 234–239 (2003).
10. C. S. Kim et al., "Determination of an optimized conversion matrix for device independent skin color image analysis," *Lasers Surg. Med.* **37**(2), 138–143 (2005).
11. D. K. Rah et al., "Objective evaluation of treatment effects on port-wine stains using L*a*b* color coordinates," *Plast. Reconstr. Surg.* **108**(4), 842–847 (2001).
12. T. Lister, P. Wright, and P. Chappell, "Spectrophotometers for the clinical assessment of port-wine stain skin lesions: a review," *Lasers Med. Sci.* **25**(3), 449–457 (2010).
13. D. Jakovels and J. Spigulis, "2-D mapping of skin chromophores in the spectral range 500–700 nm," *J. Biophotonics* **3**(3), 125–129 (2010).
14. I. Kuzmina et al., "Towards noncontact skin melanoma selection by multispectral imaging analysis," *J. Biomed. Opt.* **16**(6), 060502 (2011).
15. I. Nishidate et al., "Visualizing of skin chromophore concentrations by use of RGB images," *Opt. Lett.* **33**(19), 2263–2265 (2008).
16. J. O'Doherty et al., "Comparison of instruments for investigation of microcirculatory blood flow and red blood cell concentration," *J. Biomed. Opt.* **14**(3), 034025 (2009).
17. D. Jakovels, J. Spigulis, and L. Rogule, "RGB mapping of hemoglobin distribution in skin," *Proc. SPIE* **8087**, 80872B (2011).
18. D. Jakovels and J. Spigulis, "RGB imaging device for mapping and monitoring of hemoglobin distribution in skin," *Lith. J. Phys.* **52**(1), 50–54 (2012).
19. B. L. Diffey, R. J. Oliver, and P. M. Farr, "A portable instrument for quantifying erythema induced by ultraviolet radiation," *Br. J. Dermatol.* **111**(6), 663–672 (1984).
20. D. Kapsokalyvas et al., "Spectral morphological analysis of skin lesions with a polarization multispectral dermoscope," *Opt. Express* **21**(4), 4826–4840 (2013).
21. P. M. McNamara et al., "Tissue viability (TiVi) imaging: temporal effects of local occlusion studies in the volar forearm," *J. Biophotonics* **3**(1–2), 66–74 (2010).
22. P. Clarys et al., "Skin color measurements: comparison between three instruments: the Chromameter®, the DermaSpectrometer® and the Mexameter®," *Skin Res. Technol.* **6**(4), 230–238 (2000).
23. H. Takiwaki et al., "Quantification of erythema and pigmentation using a video-microscope and a computer," *Br. J. Dermatol.* **131**(1), 85–92 (1994).
24. B. Jung et al., "Use of erythema index imaging for systematic analysis of port wine stain skin response to laser therapy," *Lasers Surg. Med.* **37**(3), 186–191 (2005).
25. Y. Zhao, J. Tao, and P. Tu, "Quantitative evaluation of efficacy of photodynamic therapy for port-wine stains using erythema index image analysis," *Photodiagnosis Photodyn. Ther.* **10**(2), 96–102 (2013).
26. S. G. Demos and R. R. Alfano, "Optical polarization imaging," *Appl. Opt.* **36**(1), 150–155 (1997).
27. L. L. Randeberg et al., "Methemoglobin formation during laser induced photothermolysis of vascular skin lesions," *Lasers Surg. Med.* **34**(5), 414–419 (2004).
28. L. E. Dolotov et al., "Design and evaluation of a novel portable erythema-melanin-meter," *Lasers Surg. Med.* **34**(2), 127–135 (2004).

Dainis Jakovels received his master's degree in medical physics in 2009 from Riga Technical University. Now he is a PhD candidate in medical physics at University of Latvia. His main research interests are light and tissue interaction, spectral imaging, skin chromophore mapping and laser speckle imaging.

Ilona Kuzmina received his doctoral degree in medical physics from University of Latvia in 2011. Her main research interests are skin phantoms, diagnostics of skin lesions by contact diffuse reflectance, and multispectral imaging.

Anna Berzina received her master's degree in general medicine in 2006 from Riga Stradins University and received dermatovenerologist's certificate from the University of Latvia in 2010. Now she works as a dermatologist in the Clinic of Laserplastics in Riga, Latvia. Her main interests in medicine are skin health and appearance improvement with laser treatment options, as well as diagnostic and therapeutical innovations in the field of skin diseases.

LaumaValeine received her master's degree in general medicine in 2006 from Univeristy of Latvia and received dermatovenerologist's certificate from the University of Latvia in 2009. Now she works as a dermatologist in the Beauty Clinic "4th Dimension" in Riga, Latvia. Her main interests in medicine are aesthetic laser treatment options of skin and novel optical techniques in dermoscopy.

Janis Spigulis is professor at physics department and head of the Biophotonics Laboratory at Institute of Atomic Physics and Spectroscopy, University of Latvia. His current research interests are related to skin optics and its use as a tool for noninvasive clinical diagnostics and monitoring